

## Inelastic $J/\psi$ helicity distributions

---

**Alessandro Bertolin\***

*on behalf of the ZEUS Collaboration*

*INFN - Sezione di Padova*

*E-mail: bertolin@pd.infn.it*

The  $J/\psi$  decay angular distributions have been measured in inelastic photoproduction in  $ep$  collisions with the ZEUS detector at HERA, using an integrated luminosity of  $468 \text{ pb}^{-1}$ . The range in photon-proton centre-of-mass energy,  $W$ , was  $50 < W < 180 \text{ GeV}$ . The  $J/\psi$  mesons were identified through their decay into muon pairs. The polar and azimuthal angles of the  $\mu^+$  were measured in the  $J/\psi$  rest frame and compared to theoretical predictions at leading and next-to-leading order in QCD.

*XVIII International Workshop on Deep-Inelastic Scattering and Related Subjects*

*April 19 -23, 2010*

*Convitto della Calza, Firenze, Italy*

---

\*Speaker.

## 1. Introduction

In the HERA photoproduction regime, where the virtuality of the exchanged photon is small, the production of inelastic  $J/\psi$  mesons is dominated by boson-gluon fusion: a photon emitted from the incoming lepton interacts with a gluon coming from the proton to produce a  $c\bar{c}$  pair which subsequently forms a  $J/\psi$  meson. Production of  $J/\psi$  through boson-gluon fusion can be calculated using perturbative Quantum Chromodynamics (pQCD) in the colour-singlet (CS), in the non-relativistic QCD (NRQCD) and in the  $k_T$ -factorisation frameworks.

In the CS approach, only the colourless  $c\bar{c}$  pair produced in the hard subprocess can lead to a physical  $J/\psi$  state. In the NRQCD approach, a  $c\bar{c}$  pair emerging from the hard process in a colour-octet (CO) state can also evolve into a  $J/\psi$  state with a probability proportional to universal long-distance matrix elements (LDME) that are obtained from experiment. In the  $k_T$ -factorisation approach, the effects of non-zero transverse momentum of the incoming parton are taken into account. Cross sections are then calculated in the CS approach as a convolution of unintegrated (transverse-momentum dependent) parton densities and leading-order (LO) off-shell matrix elements.

The polar and azimuthal distributions of the  $J/\psi$  decay leptons in the  $J/\psi$  rest frame, the helicity distributions, may be used to distinguish between CS and CO models [1]. Helicity distribution measurements have already been performed by the ZEUS [2] and H1 [3, 4] collaborations. The data sample of this study [5] includes the data used in the previously published ZEUS analysis [2] and corresponds to an increase in statistics of a factor of 12.

## 2. Data analysis

$J/\psi$  mesons were identified using the decay mode  $J/\psi \rightarrow \mu^+\mu^-$ . The online and offline selections as well as the reconstruction of the kinematic variables closely follow a previous analysis [2]. The transverse momentum,  $p_T$ , of the  $J/\psi$  candidate was required to be larger than 1 GeV. The photon-proton centre-of-mass energy  $W$  was restricted to the range  $50 < W < 180$  GeV. In addition, events were required to have an energy deposit larger than 1 GeV in a cone of  $35^\circ$  around the forward direction (excluding possible calorimeter deposits due to the decay muons). According to Monte Carlo (MC) simulations, these requirements completely reject exclusively produced  $J/\psi$  mesons ( $ep \rightarrow epJ/\psi$ ) as well as proton-diffractive events ( $ep \rightarrow eYJ/\psi$ ) in which the mass of the proton dissociative state,  $M_Y$ , is below 4.4 GeV. To further reduce diffractive background, events were also required to have at least one additional track with a transverse momentum larger than 0.125 GeV and pseudorapidity  $|\eta| < 1.75$ .

The following other sources of  $J/\psi$  mesons, which were classified as background in the present analysis, were estimated either from MC models or previous measurements:

- diffractive production of  $J/\psi$  mesons with proton dissociation: the overall contribution of this background is 6%; it is largest in the lowest  $p_T$  bin ( $1 \leq p_T \leq 1.4$  GeV), where it is 7.5%, and in the highest  $z$  bin ( $0.9 \leq z \leq 1$ ), where it is 66%;
- $J/\psi$  mesons originating from  $B$ -meson decays: 1.6% of the observed  $J/\psi$  events were from  $B$ -meson decays; the fraction is largest in the highest  $p_T$  bin ( $4.2 \leq p_T \leq 10$  GeV), where it is equal to 6.3%, and in the lowest  $z$  bin ( $0.1 \leq z \leq 0.4$ ), where it is 8.4%

- $J/\psi$  from  $\psi'$  decays: this contribution is expected to be around 15%, as obtained using the direct measurement of the  $\psi'$  to  $J/\psi$  cross section ratio [2] and the branching ratio of the  $\psi'$  to  $J/\psi$ .

Although the relative rate of each process could be estimated, the helicity distributions of these  $J/\psi$  sources are poorly known, so these contributions were not subtracted.

The helicity analysis was performed in the so-called “target frame” [1]. The polar and azimuthal angles of the  $\mu^+$  in this frame are denoted  $\theta^*$  and  $\phi^*$ . The differential cross sections in  $\theta^*$  and  $\phi^*$  can be parametrised as [1]:

$$\frac{d\sigma}{d\cos\theta^*} \propto 1 + \lambda \cos^2\theta^*, \quad (2.1)$$

$$\frac{d\sigma}{d\phi^*} \propto 1 + \frac{\lambda}{3} + \frac{\nu}{3} \cos 2\phi^*, \quad (2.2)$$

where  $\lambda$  and  $\nu$ , the polar and azimuthal angular parameters, are functions of  $p_T$  and  $z$ . The  $\lambda$  and  $\nu$  parameters were determined in bins of  $z$  and  $p_T$ , each time integrating over the other variable. As a function of  $p_T$ , the integration range for  $z$  was set to  $0.4 < z < 1$ , thereby avoiding the region  $0.1 < z < 0.4$  where the ratio of signal to combinatorial background is rather poor. The integration range in  $p_T$  started at  $p_T = 1$  GeV.

The HERWIG MC generator-level distributions  $dN/d\cos\theta^*$  ( $dN/d\phi^*$ ) were re-weighted according to Eq. 2.1 (2.2) within a search grid of  $\lambda$  ( $\nu$ ) values. For each re-weighted distribution, the value of  $\chi^2$  was calculated from a comparison to the data. The  $\lambda$  ( $\nu$ ) value providing the minimum  $\chi^2$ ,  $\chi_{\min}^2$ , was taken as the central value. The parameter values with  $\chi^2 = \chi_{\min}^2 + 1$  were used to calculate the statistical uncertainties. Equation 2.1 was first used to extract  $\lambda$ , and then  $\lambda$  was inserted into Eq. 2.2 to extract  $\nu$ .

### 3. Results

The values of the parameter  $\lambda$  are shown as a function of  $p_T$  and  $z$  in Figs. 1a) and b), respectively; the values of the parameter  $\nu$  are displayed in Figs. 2a) and b).

The data are compared to various theoretical predictions for photoproduction, at  $Q^2 = 0$ . These predictions do not consider the polarisation due to  $J/\psi$  coming from  $\psi'$  decays,  $B$ -meson decays and from diffractive processes. The curves identified by the label LO CS show the LO prediction in the CS framework including both direct and resolved<sup>1</sup> processes. The two lines identified by the label LO +  $k_T$  (JB) and LO +  $k_T$  (dGRV), represent the predictions of a  $k_T$ -factorisation model using two different unintegrated gluon distributions and including only direct processes. The band identified by the label NLO CS represents the predictions of a NLO calculation including only direct processes. The width of the band gives the uncertainties of the calculation due to variations of the renormalisation and factorisation scales. It stops at  $z = 0.9$  because no reliable predictions can be obtained near  $z = 1$  for this fixed-order calculation. The band identified by the label LO CS+CO shows a LO prediction including direct and resolved processes in the NRQCD approach

<sup>1</sup>In these resolved processes, the incoming photon does not couple to the  $c$  quark directly, but via its hadronic component. They are expected to contribute mainly to the region of  $z < 0.4$ .

and hence involving CS plus CO states. The width of the band results from the uncertainties in the values of the CO matrix elements. In Figs. 1a) and 2a), with  $z$  integrated up to  $z = 1$ , the LO CS+CO cross section is CO dominated.

The NLO CS calculation for  $p_T > 1$  GeV suffers from large scale uncertainties. In order to avoid this problem, measurements and calculations were repeated increasing the  $p_T$  cut first to 2 GeV and then to 3 GeV. In Figs. 3a) and b) the  $\lambda$  and  $\nu$  parameters, respectively, are shown as a function of  $z$  for  $p_T > 2$  GeV, while in Figs. 3c) and d) the same parameters are displayed for  $p_T > 3$  GeV. The NLO CS calculation, also shown in these figures, has now smaller uncertainties, but the agreement with the data is only satisfactory for the  $\nu$  parameter. Sizeable discrepancies remain for the  $\lambda$  parameter both for  $p_T > 2$  GeV and  $p_T > 3$  GeV.

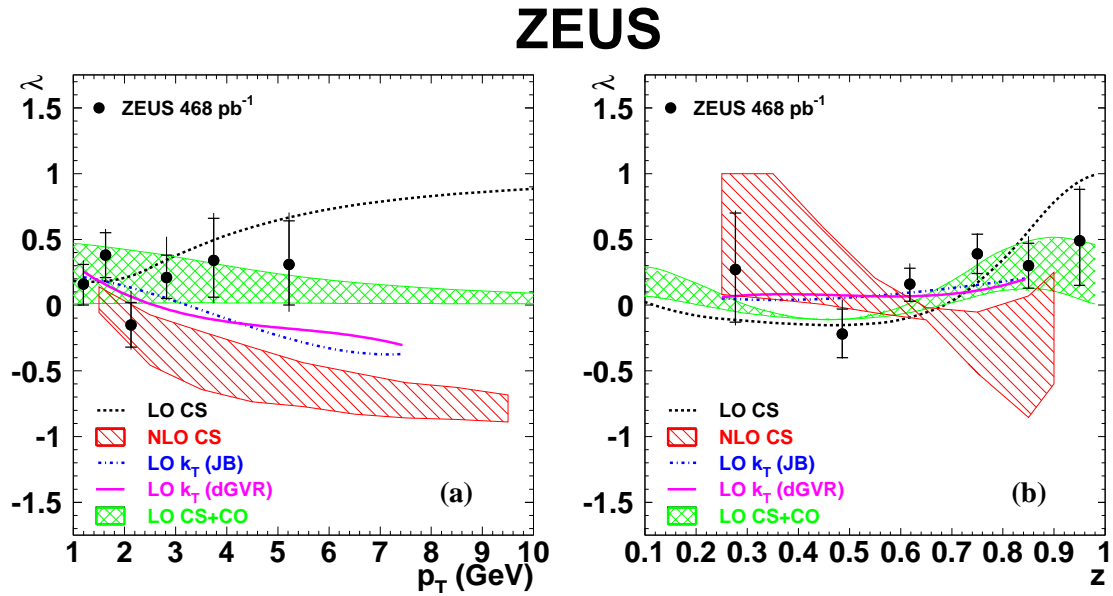


**Figure 1:** The helicity parameter  $\lambda$ , measured in the target frame, as a function of (a)  $p_T$ , and (b)  $z$ . The measurement is performed in the kinematic range  $50 < W < 180$  GeV,  $0.1 < z < 1$  and  $p_T > 1$  GeV. The measurement as a function of  $p_T$  is restricted to the kinematic range  $0.4 < z < 1$ . The inner (outer) error bars correspond to the statistical (total) uncertainty. The theoretical curves are described in the text.

#### 4. Conclusions

The  $J/\psi$  helicity distributions in the inelastic photoproduction regime have been measured using a luminosity of 468 pb<sup>-1</sup>. The  $J/\psi$  helicity parameters  $\lambda$  and  $\nu$  were extracted in the target frame as a function of the transverse momentum and of the inelasticity of the  $J/\psi$ . The results were compared to LO QCD predictions in the colour-singlet, colour-singlet plus colour-octet and  $k_T$  factorisation frameworks. A recent NLO QCD prediction in the colour-singlet framework was also considered. Even though the experimental and theoretical uncertainties are large, none of the predictions can describe all aspects of the data.

#### References

- [1] M. Beneke, M. Krämer and M. Vanttinen, Phys. Rev. **D 57**, 4258 (1998);

## ZEUS

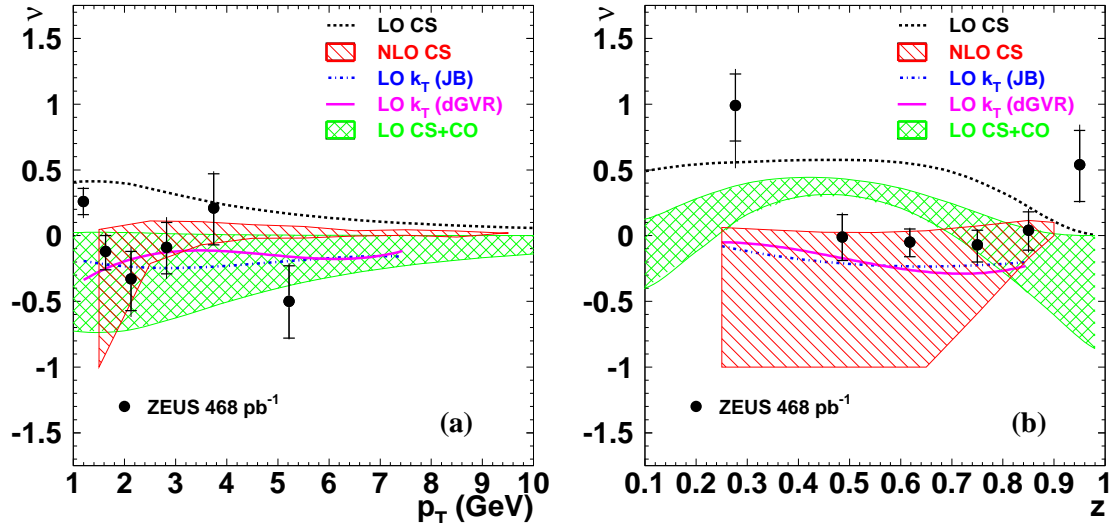


**Figure 2:** The helicity parameter  $\nu$ , measured in the target frame, as a function of (a)  $p_T$ , and (b)  $z$ . The measurement is performed in the kinematic range  $50 < W < 180$  GeV,  $0.1 < z < 1$  and  $p_T > 1$  GeV. The measurement as a function of  $p_T$  is restricted to the kinematic range  $0.4 < z < 1$ . The inner (outer) error bars correspond to the statistical (total) uncertainty. The theoretical curves are described in the text.

- [2] S. Chekanov *et al.*, Eur. Phys. J. C **27**, 173 (2003);
- [3] C. Adloff *et al.*, Eur. Phys. J. C **25**, 25 (2002);
- [4] F. D. Aaron *et al.*, DESY-09-225, arXiv:1002.0234, submitted to EPJC;
- [5] S. Chekanov *et al.*, JHEP12 (2009) 007.

# ZEUS

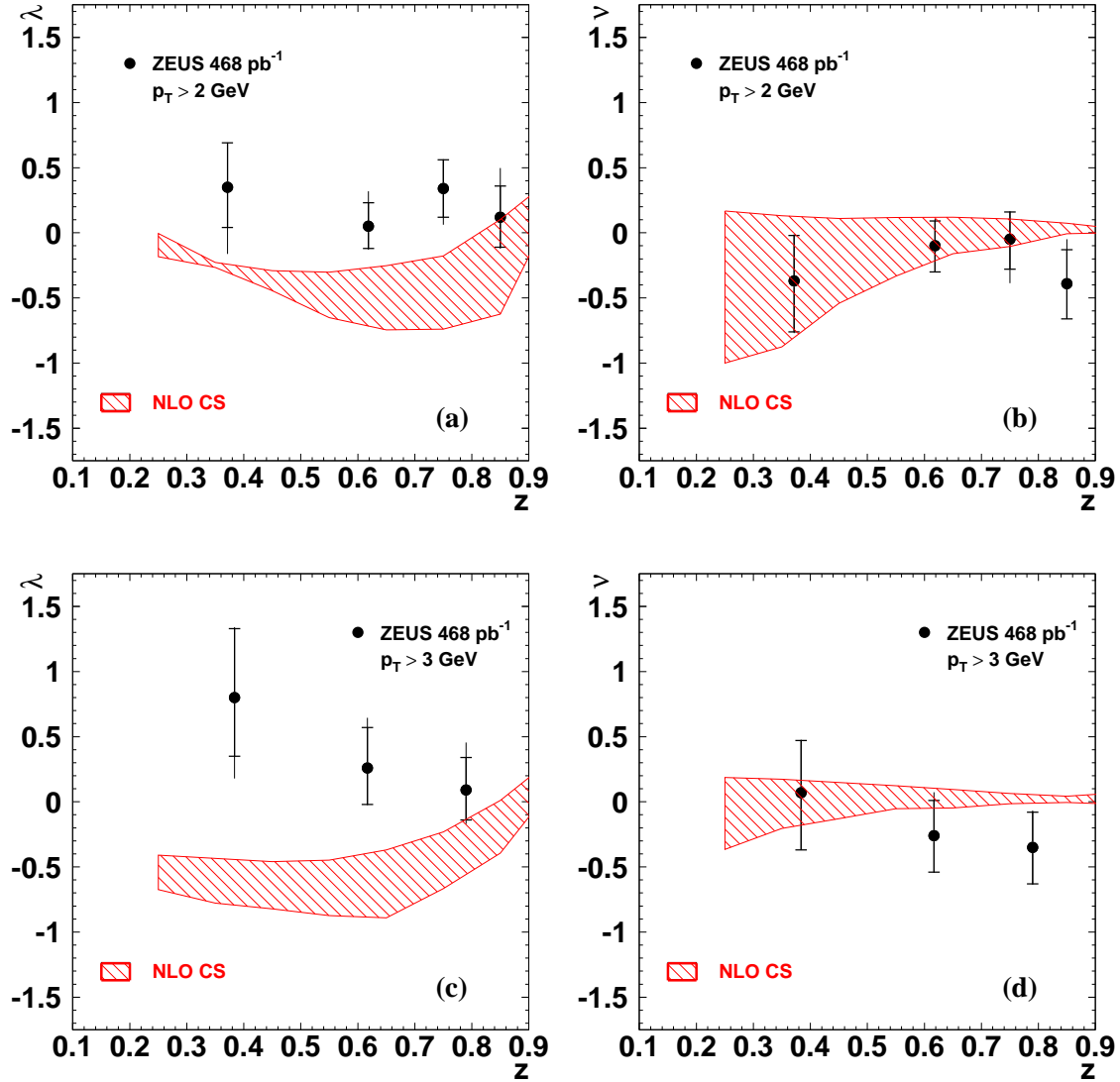


**Figure 3:** Distributions of the helicity parameters (a), (c)  $\lambda$  and (b), (d)  $\nu$  as a function of  $z$ , measured in the target frame, for  $50 < W < 180$  GeV,  $0.1 < z < 0.9$  and (a), (b)  $p_T > 2$  GeV and (c), (d)  $p_T > 3$  GeV. The inner (outer) error bars correspond to the statistical (total) uncertainty. The theoretical bands are described in the text.